

Thermal deformations of cutting tools: measurement and numerical simulation

Ulrich Semmler · Michael Bräunig ·
Welf-Guntram Drossel · Gerhard Schmidt ·
Volker Wittstock

Received: 5 December 2013 / Accepted: 19 March 2014 / Published online: 2 April 2014
© German Academic Society for Production Engineering (WGP) 2014

Abstract Challenges for machining include greater and greater material removal rates coupled with an increase in the use of difficult to machine materials, as well as environmental-friendly dry or minimum quantity lubrication machining, small manufacturing batches and frequently changed manufacturing orders. These trends are accompanied by high temperatures in the machining process and large, variable heat flows causing thermo-elastic displacements of the tool, the workpiece and the clamping devices. Although the displacements are small, in the range of a few micrometers, they have assumed more and more importance because of growing requirements for manufacturing accuracy. Thermo-elastic displacements of the tool due to

heat flow during machining are investigated and analysed in this paper. Temperatures and displacements are measured on a test bed equipped with measuring instruments. The identification of the thermal boundary and contact conditions is supported by finite element models. Knowledge of the heat flows resulting from the machining process is a prerequisite for control of and compensation for displacements. Since these heat flows either cannot be measured or can only be measured with enormous effort, heat flows are determined by means of numerical simulation of the machining process itself. This strategy has been previously used as a systematic approach for turning in orthogonal cutting conditions. However, further investigations are needed for oblique turning conditions, milling and drilling operations.

The topic is part of the Collaborative Research Centre funded by the German Research Association DFG focusing on thermo-energetic design of machine tools.

U. Semmler (✉) · W.-G. Drossel · G. Schmidt
Fraunhofer Institute for Machine Tools and Forming Technology
IWU, Chemnitz, Germany
e-mail: ulrich.semmler@iwu.fraunhofer.de
URL: <http://www.iwu.fraunhofer.de>

W.-G. Drossel
e-mail: welf-guntram.drossel@iwu.fraunhofer.de
URL: <http://www.iwu.fraunhofer.de>

G. Schmidt
e-mail: gerhard.schmidt@iwu.fraunhofer.de
URL: <http://www.iwu.fraunhofer.de>

M. Bräunig · V. Wittstock
Chemnitz University of Technology, Chemnitz, Germany
e-mail: michael.braeunig@mb.tu-chemnitz.de
URL: <http://www.tu-chemnitz.de>

V. Wittstock
e-mail: volker.wittstock@mb.tu-chemnitz.de
URL: <http://www.tu-chemnitz.de>

Keywords Cutting tool · Thermal displacements · Temperature measurement · Finite element modelling · Heat source

Abbreviations

TCP Tool centre point
HPC High performance cutting
FE Finite element
WP Workpiece
R&D Research and development

1 Introduction

In addition to static and dynamic machine tool characteristics, heat flows inside the machine affect the position of the tool centre point (TCP) and, consequently, positioning accuracy [1]. Machining heat is a substantial heat source in

the overall system of the machine tool. Heat is created immediately in the machined material (forming heat) and in the contact zone between tool and workpiece (WP) (frictional heat) and causes thermo-elastic deformations of tool and WP. It dissipates, in the form of heat flow, through the tool chuck into the spindle, and through the WP and the clamping system into the machine table.

The demands of high manufacturing accuracy are opposed to these thermo-elastic deformations, which are reinforced by the trend towards high performance cutting (HPC) and dry machining or minimum quantity lubrication. The conflicts resulting from the need for accuracy, productivity and ecological requirements are exacerbated by small manufacturing batches, changing manufacturing orders and tool changes, as well as shut downs of base load power design to conserve energy. As a result, it is frequently impossible in machining to arrive at a thermally stable machine state.

2 Aims and approach

In the Collaborative Research Centre (SFB) Transregio96 focused on “thermo-energetic design of machine tools” [2], heat flows are being investigated in order to obtain a better thermo-energetic design of machines and to find strategies to avoid, reduce, correct, or compensate for TCP deviations due to thermal influence. The thermal processes in the tool–chuck system and the WP clamping system are being investigated within the A01 subproject entitled “Deformation of tool and clamping device” of the SFB. This paper deals with the tool–tool holder system.

An end mill completely made of carbide, fixed in various clamping chucks with steep taper SK40, was the tool used. To determine the consequences of the increase in tool temperature on the position of the TCP, long-term experiments were carried out using these tools in an air-conditioned chamber. For these tests, extensive temperature and displacement measuring techniques were utilised. The tool was heated at its tip in different ways. Section 3 describes the experimental setup and the measurement techniques used.

The real size of the heat source and the parameters of the heat transfer into the environment or between tool and chuck were the unknown values. To identify these unknown values, finite element (FE) models were designed, and the parameters were adjusted using the measured temperature and deformation parameters (Sect. 4.1). Afterwards, it was possible to use these verified models to simulate arbitrary thermal loads, varying in magnitude and sequence in time, without performing time-consuming and labour-intensive experiments. These

explorations are aimed at simplified models with real-time capability, providing the current correction values immediately during manufacturing.

The heat source in a real machining process derives from the forming energy transformed during chip formation and the frictional heat generated by the contact of tool and WP or chip. There are available various empirical and analytical models for temperature distribution in the chip forming and frictional contact zone (for instance [3]). However, all of them are based on simplified model assumptions and are, for that reason, inexact. Thus, they are conditionally transferable to most machining processes. Direct measurement of heat generated in the machining process is also possible under simplified process conditions, but only when using adequately designed tools and workpieces. Furthermore, it is very costly in terms of measurement equipment. An overview is provided in [4]. The heat flows resulting from the heat content generated are important for the thermo-elastic deformations considered here. In the literature, statements predicting the share of heat dissipating into tool, chips and WP are widely divergent. The partition relevant for the thermal impact on the tool varies—depending on the machining process—from 1 to 20 % [5–8]. The percentage of heat dissipating into the chips rises as cutting speed increases, whereas that of heat dissipation into the tool and WP goes down.

The contact heat transfer coefficients between tool and chuck cannot be measured directly. The results gained in the subproject B02 of the Transregio96 [9] project were introduced into the FE model. However, it should be noted that they do not play a significant part in the heat flow out from the tool (Sect. 5).

Finite element modelling of the machining process as explained in Sect. 4.2 makes it possible to determine the temperature distribution inside the WP, considering the chip and the WP surface generated, and inside the tool, both in terms of amount and distribution, by making use of an additional software tool for heat flow analysis. This methodology was employed for high-performance drilling in [10]. An 8–11.3 % heat flow partition dissipated into the tool was calculated and shown in experiments.

Finite element simulation is based on models of materials data and of friction on contact faces. The results demonstrated are related to the steel material AISI-1045 and are based on well-established values from the literature. In order to validate the model, experiments were carried out in parallel on a test bed for fundamental research at the RWTH Aachen [11].

The results derived from measurements and simulation are summarised and evaluated in Sect. 5. Concluding remarks and a look at continuing R&D activities are presented in Sect. 6.

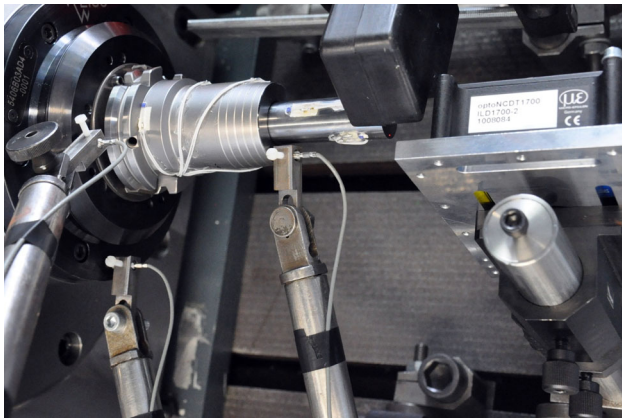


Fig. 1 Tool and hydro strain chuck in motor spindle, with installed measuring devices and inductive heat source

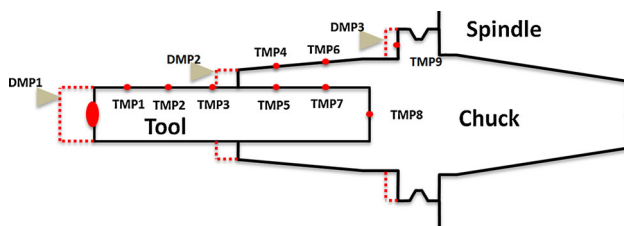


Fig. 2 Measuring points for temperature (TMP) and displacement (DMP) (stationary tool, schematic view)

3 Experiments: test set up and installation for measurement

A test bed, consisting of an encapsulated machine bed and a stand for the motor spindle, is placed in an air-conditioned lab-space. The spindle can be mounted horizontally or vertically, whereas—in the future—the spindle position will play an important role for experiments with lubricant cooling. A cutting fluid system makes possible future thermo-energetic investigations under the influence of coolants. The temperature was measured by resistance thermometers in thin-film technology (Fig. 1). To carry out the experiments under the conditions of rotation, wiring is guided through the tool's cooling channels. The measured values are transmitted by means of collector rings. In the measurements, dummy-tools in the form of carbide cylinders with cooling channels are used rather than finished-ground tools. The points at which temperature and displacement were measured are located at the tool and chuck positions marked in Fig. 2. The temperature was also measured at another two points (measuring points TMP5 and TMP7) on the chuck near the tool–chuck contact surface.

For stationary tools, displacement was measured by inductive displacement transducers. To prevent the measurements from being affected by heating, displacement

was measured at the tool tip by means of a laser distance measuring system. The measurement setup for a hydraulic chuck mounted onto the spindle, fitted with a carbide cylinder with a dummy-tool, is shown in Fig. 1. Contactless measuring systems based on eddy current principle were deployed for the rotating tool. A thermal imaging camera was an additional attachment, used, in particular, for rotatory operation.

Heating of the tool due to machining was simulated in the test bed by heating at the tool tip. In stationary mode, either a heating cartridge was placed at the tip or the increase in temperature was achieved through inductive heating. In the rotatory mode, only inductive heating is feasible, where the measuring setup permits values of maximal 1,000 revolutions per min. For a more detailed description of test hardware and measuring equipment, see [12].

Until now, long-term measurements with phases of 6 h for heating and 10 h for cooling down have only been executed for stationary carbide cylinders with cooling channels with chucks of the following types: thermo shrink-fit chucks, hydraulic chucks, Weldon chucks. For the rotatory mode, measurements were done only for the hydro strain chuck.

4 Finite element models

4.1 Finite element models for thermal deformation of tool–chuck systems

In the measurements, heat flow content brought into the tool through heating, heat transfer into the environment and the contact heat transfer coefficients between tool and chuck are non-measurable parameters and thus a priori unknown. To determine these parameters based on the measurements, FE analysis models for the applied tools (real tool and dummy-tool) and for all chucks were generated by means of the FE system MSC.MARC® [13]. Figure 3 elucidates the part geometry and an FE model for the shrink-fit chuck with the semi-finished tool.

The thermo-elastic and thermo-physical material parameters of the K40 carbide used for the tool and the chuck material 1.2342 (X38CrMoV5-1) were chosen from material databases and manufacturer specifications.

The thermal boundary and contact conditions are illustrated in Fig. 4. Heat source modelling either assumes constant temperature in the heating rod or uses the heat flows along the front face of the semi-finished tool, where unknown parameters are used at the beginning. These unknown parameters have to be matched with the values obtained in the subsequent experiments.

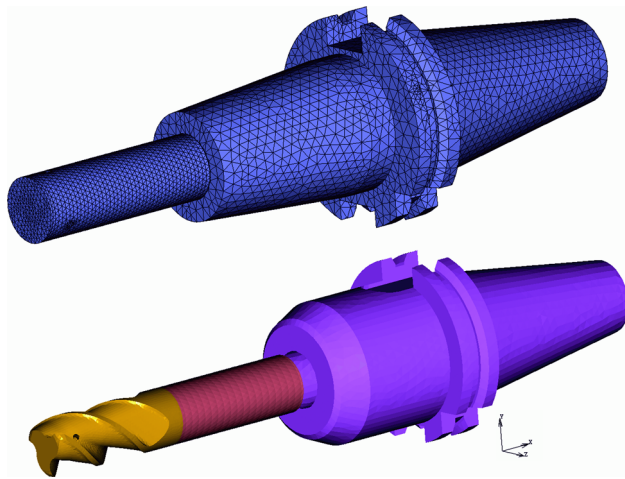


Fig. 3 Finite element analysis models of tools and chucks—examples (top carbide cylinder with dummy-tool, bottom end mill in Weldon-type chuck)

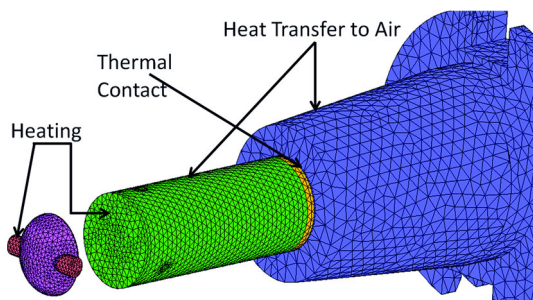


Fig. 4 FE model of the dummy-tool in the shrink-fit chuck: thermal boundary and contact conditions (heater cartridge with thermal interface grease are represented separately)

4.2 Finite element machining process model for determination of heat source

To evaluate the temperature profiles in the tool–WP system and the resulting deformations, which affect the location of the TCP, one has to quantify the heat flows emitted by the machining process on the machine tool.

Numerical simulation of the cutting process is utilised here, since heat flows either cannot be measured in-process or can only be determined with enormous effort. Furthermore, empirical or analytical models are insufficient [14]. In simulation, the temperature fields in the WP, the tool and the chip can be calculated over the whole period of time. An autonomous software tool independent of the FE program was created to determine the content and distribution of heat inside the tool, the WP and the chip by means of calculated temperature fields. The heat flows were obtained from the changes in heat content. First, simplified 2D chip formation models were simulated to quantify the extent to which the

heat flows depend on tool and WP material, cutting parameters, such as cutting speed and feed, and tool geometry, specified by cutting edge radius, rake and clearance angles. In the beginning, 2D chip formation models (turning in orthogonal cutting conditions and milling as 2D planing with variable depth of cut) were used (see Fig. 5). The numbers 0.025, 0.0036 and 0.0012 in Fig. 5 are the average element edge length in the meshing windows.

The simulation runs were executed with the MSC.MARC[®] and DEFORM[™] [15] systems, using AISI-1045 as the WP material and K40 carbide as the tool material. The Johnson–Cook model proposed by Jaspers and Dautzenberg [16] is frequently utilised for FE models of AISI-1045 machining processes and is well established. For this reason, this model was used as the yield law for temperatures that typically occur in machining processes and strain rates, assuming $A = 553.1$, $B = 600.8$, $C = 0.0123$, $n = 0.234$, $m = 1$ [16].

To model the frictional contact, the shear friction method with a coefficient of friction of $\mu = 0.6$ was employed. The parameter μ is important for frictional heat, which, however, is minor in comparison with the heat generated in the deformation. Furthermore, the parameter μ influences the chip shape, which is characterised by the direction of chip flow, chip curvature and chip compression, as well as the thrust force defined as the vectorial sum of passive force and feed force. This, however, is not part of these investigations.

There are no certain measured values for the contact heat transfer coefficients α_{tool_WP} . As a default, the Machining Wizard of DEFORM sets $\alpha_{tool_WP} = 45,000 \text{ W/m}^2/\text{K}$. In [8], a significantly higher value— $10^6 \text{ W/m}^2/\text{K}$ —was determined in experiments. This high value is the result of a procedure that is not physically consistent, as conceded by the authors. As shown by comparative calculations, when this value is included, the ratio of the heat content dissipating into the tool doubles. However, further investigations are required to validate this statement.

In the very time-consuming simulations of chip formation, it is only possible to efficiently calculate very small time intervals: as a rule, up to the formation of a stationary flow chip or, in the case of laminated chips, until a periodically repeating chip form has been established. Generally, this way, a thermal equilibrium in tool and WP is not achieved. Only a small part of the tool and WP is modelled. When omitting heat exchange in the model—both with the environment and, exceeding the model boundaries, also with the remaining parts of the tool and the WP (adiabatic thermal boundary conditions at all boundaries of the modelling domains according to Fig. 6)—we can then calculate the accumulated heat content W_{Tool} .

Fig. 5 FE model for turning in orthogonal cut (2D model) with mesh refinement windows

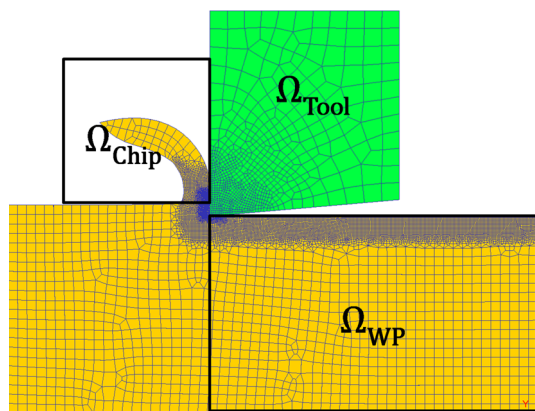
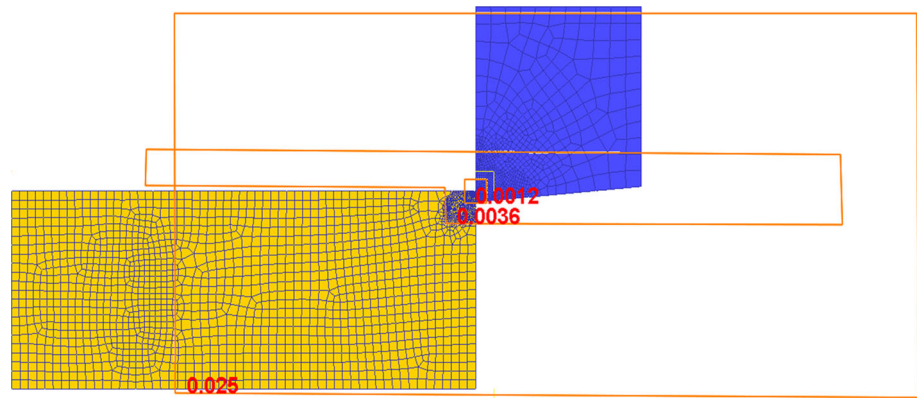


Fig. 6 Integration domains for heat flow calculation

$$W_{Tool} = \sum_{e_{Tool}} \int_{\Omega_e} \rho(T) c_p(T) T d\Omega \quad (1)$$

as the sum over all elements e_{Tool} belonging to the domain Ω_{Tool} and, for two successive time steps t_{i-1} and t_i , the heat flow into the domain Ω_{Tool} as follows

$$P_{Tool}(t_i) \approx \frac{W_{Tool}(t_i) - W_{Tool}(t_{i-1})}{t_i - t_{i-1}} \quad (2)$$

Analogous equations are valid for W_{WP} , P_{WP} , W_{Chip} and P_{Chip} , respectively. The integrating procedures according to (1) and (2) were performed based on the meshes and node temperatures stored during FE simulation. Making use of the heat flows calculated as above mentioned, it was possible to quantify temperature development in the tool for greater periods of time by means of the models described in Sect. 4.1, as well as, analogously, for the WP. Assuming intermittent cutting, it is necessary to scale the heat source using the ratio of engagement time of the cutting edge to the total time, which is then in the case of more than one cutting edge to be multiplied by the number of cutting edges.

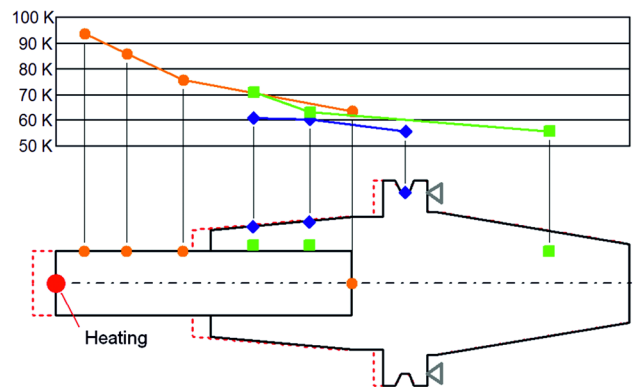


Fig. 7 Measured thermo-elastic state for shrink-fit chuck after 6 h of heating time

5 Results and discussion

5.1 Measurement of tool–chuck deformations

The measured results for stationary tools are shown as an example. In the setup, the chucks are not clamped into the spindle, but placed in the area of the spindle interface in a thermally insulated way. The thermo-elastic equilibrium for the shrink-fit chuck, which is obtained at the end of heating time after 6 h, is illustrated in Fig. 7.

Similar temperature profiles and elongations were produced for the other chuck types. In the case of the Weldon chuck, temperatures were slightly higher (max. 2 K) on the side away from the straining screw due to the asymmetric design of the chuck.

5.2 Matching of the FE model for thermal boundary and contact conditions

The thermal boundary and contact conditions were matched for the shrink-fit chuck. The closest match with the measurements was established for a heat transfer coefficient α_{Air} of 8 W/m²/K into the environment and a heat flow of 8.1 W across the tool front face. For these

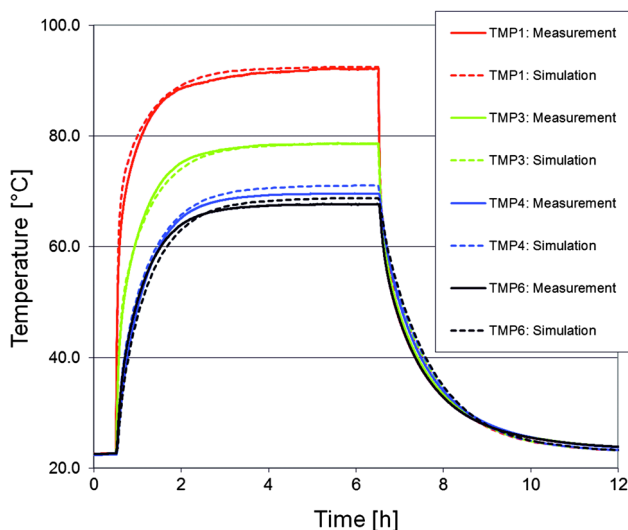


Fig. 8 Comparison of measured and simulated temperatures in selected measuring points

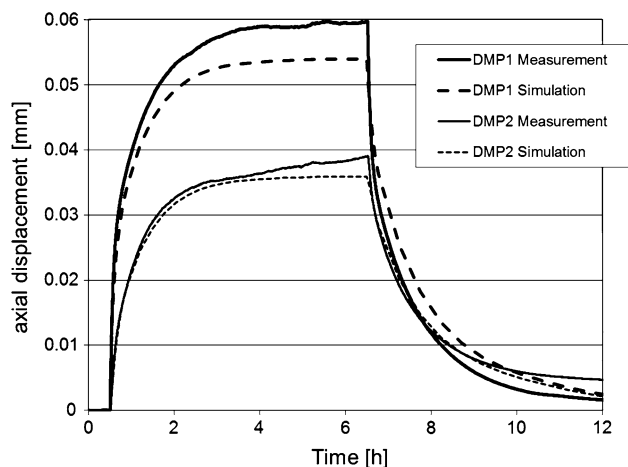


Fig. 9 Comparison of measured versus simulated displacements

parameters, the measured values in comparison with the simulated temperature values, as well as the axial displacement at the tool tip and the chuck front face (measuring points for temperatures and displacement according to Fig. 2) are shown in Figs. 8, 9.

The absolute deviations between the measured and simulated values were 2 K for temperatures, and 7 μm for displacement.

Since the tool and chuck surfaces have a low roughness and normal compressive stresses are high, a heat transfer coefficient $\alpha_{therm} = 12,000 \text{ W/m}^2/\text{K}$ was applied in accordance with the investigations carried out in subproject B02 [2]. However, the amount of the parameter does not significantly affect the temperature and displacements values in the tool–chuck system, as evidenced by simulations performed with different α values (Fig. 10, for cross sections see Fig. 2).

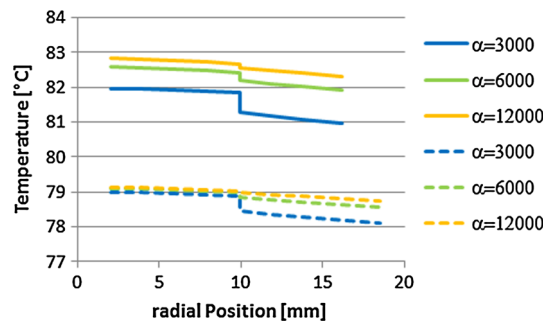


Fig. 10 Temperature discontinuities in the contact between tool and chuck, calculated in the cross sections TMP4–TMP5 and TMP6–TMP7 (see Fig. 2) for different heat transfer coefficients

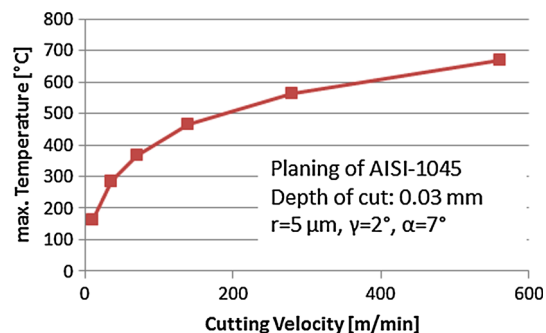


Fig. 11 Maximal temperatures at rake face calculated for different cutting speed values

5.3 Heat source obtained in the simulation of the machining process

The simulation results summarised below are achieved based on the methodology explained in Sect. 4.2 for machining of AISI-1045 steel. The results rely on the following model parameters: cutting speed $v_c = 10, 35, 70, 140, 280, 560 \text{ m/min}$, depth of cut $h = f_z = 30 \mu\text{m}$, cutting edge radius $r = 5 \mu\text{m}$, tool rake angle $\gamma = 2^\circ$, tool clearance angle $\alpha = 7^\circ$ and meet the conditions of precision cutting.

The simulation results substantiate the widely known phenomenon in which increased cutting speed in the machining process clearly increases temperatures, while the cutting forces decrease slightly (Figs. 11 and 12).

With regard to the heat balance of the machining process, the increase in heat generated in the machining process is approximately proportional to the increase in cutting speed (Fig. 13). At the same time, the percentage of process heat transferred into the chips clearly rises to approximately 70 % for $v_c = 560 \text{ m/min}$ (see Fig. 14), whereas the ratio dissipated into the WP diminishes to approx. 26 %. For the impacts on the tool–chuck system

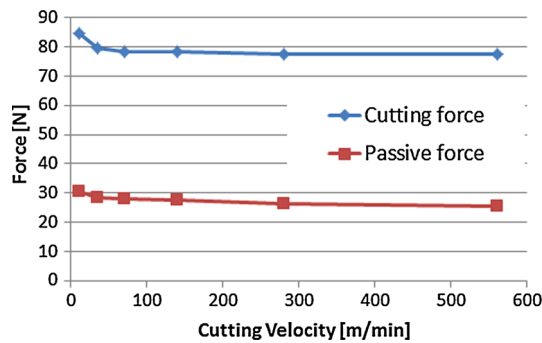


Fig. 12 Cutting forces calculated for different cutting speed values

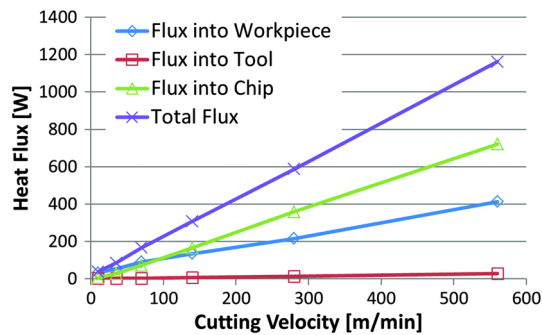


Fig. 13 Calculated heat flows calculated for different cutting speeds

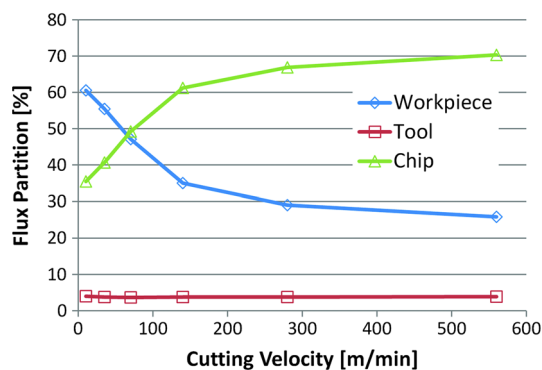


Fig. 14 Calculated percentage heat flow distribution for different cutting speed values

which are the focus of consideration in this paper, the tool partition, which only slightly changes itself at increasing cutting speed and is around 4 %, is important. In the authors’ view, the heat transfer coefficient of $10^6 \text{ W/m}^2/\text{K}$ used in the simulations is set too high. The partition is only about 2 % when using the DEFORM value of $45,000 \text{ W/m}^2/\text{K}$.

In order to validate the cutting simulations a series of 2D cutting experiments with AISI-1045 WPs was done. Table 1 shows the satisfactory match on forces and chip

Table 1 Comparison of simulated forces and chip curling radii with measurements

No.	f_z (mm)	v_c (m/min)	Cutting force (N)		Chip curling radius (mm)	
			Exp.	Sim.	Exp.	Sim.
C1	0.1	500	192	180	0.5	0.5
C2	0.1	750	152	178	0.3	0.4
C3	0.2	250	356	360	1.5–2.0	1.2
C4	0.2	500	330	360	1.0	0.9

curling radii between experiment and simulation, whilst the temperature validation needs further investigation.

5.4 Assessment for real machining processes

The calculated heat flows are obtained from continuous 2D planing with a sectional area of chip $A_{Chip_sim} = 0.03 \text{ mm}^2$. In the case of other machining processes, the heat flows P_{sim} computed in simulation have to be scaled with the following factors or correction values

$$P_{real} = P_{sim} \cdot C_1 \cdot C_2 \cdot C_3 \cdot C_4 \cdot C_5$$

$C_1 = \frac{A_{Chip_real}}{A_{Chip_sim}}$ is applicable for other chip sectional area, $C_2 = z$ if z cutting edges are engaged, $C_3 \sim 1.5$ for 3D processes (for instance external cylindrical turning), $C_4 \sim 0.75$ for processes with variable chip area (e.g. milling) and $C_5 = \frac{t_{cut}}{t_{total}}$ for processes with interrupted cut, if the tool’s cutting edges are only temporally engaged. Both correction values C_3 and C_4 are approximated values determined in separate simulation runs. However, systematic investigations on this subject are still needed.

The specified correction value C_3 was determined for 3D external cylindrical turning compared to 2D planing in the same chip sectional area. For other processes, such as drilling and face milling, in which the cutting speeds vary along the cutting edge and the material is increasingly squeezed near the tool centre, the correction factors are still to be explored. Correction factor C_4 was determined for AISI-1045 investigated here, as well as the analysed cutting speed values in the simulation of milling (planing at variable depth of cut) in comparison with the planing of constant depth of cut.

Calculation of heat flows is aimed at commensurability of the heat sources applied for the experiments on the thermo-elastic characteristics of tools and chucks with the heat sources for real machining conditions. Let us consider, for instance, the following high-performance milling process with the milling cutter of 20 mm diameter and three cutting edges used in the experiments. Let the process parameters be $n = 2,228 \text{ min}^{-1}$ (that is $v_c = 140 \text{ m/min}$), $a_e = 5 \text{ mm}$, $a_p = 2 \text{ mm}$, $f_z = 0.05 \text{ mm}$ (that is, the real

sectional area of chip is $A_{Chip_real} = 0.1 \text{ mm}^2$). Simulation provides a heat flow of $P_{sim} = 13.1 \text{ W}$ for this cutting speed and a chip sectional area $A_{Chip_sim} = 0.03 \text{ mm}^2$. Assuming a cutting engagement $a_e = 5 \text{ mm}$, each cutting edge is engaged at an angle $\varphi_c = 60^\circ$, that is one-sixth of time. From this we derive

$$C_1 = 3.33, \quad C_2 = 3, \quad C_3 = 1.5, \quad C_4 = 0.75, \\ C_5 = 0.167, \quad P_{real} = 24.5625 \text{ W}.$$

This power of heat source corresponds to approximately the threefold value of the heat source used in the long-term experiments. In real processes, these thermal loads mostly occur over shorter time spans, but, for instance when machining of titanium integral components, this loads lasts so long that the displacement values measured in the experiments and simulated correspond to real values of TCP displacement resulting from machining.

6 Conclusions and outlook

Heat flows from thermal energy generated in the machining process cause notable thermo-elastic displacements of the TCP, which have to be taken into account and which must be corrected or compensated for in the manufacturing process. Using a milling cutter as the tool, these thermo-elastic displacements were measured for different chucks in a test bed, and the parameters were matched using FE simulation. The heat flows appearing in the process were calculated and analysed by numerical simulation of the machining process and by analogous considerations of real manufacturing process. Until now, systematic investigations were performed only for turning in orthogonal cut for AISI-1045 material.

In ongoing investigations, the results will be extended to other materials and manufacturing processes, such as turning as non-free cutting, milling and drilling. The correction factors, hitherto determined only for exemplary models, have to be substantiated for these processes.

For heat dissipation into the WP, the corresponding heat flows can also be calculated. The methodology introduced will be implemented for the thermo-energetic impact on the system WP—clamping system.

Acknowledgments The authors would like to thank the German Research Foundation (DFG) for financial support within the Collaborative Research Centre Transregio 96 (SFB TR96).

References

1. Neugebauer R (2012) Werkzeugmaschinen—Aufbau Funktion und Anwendung von spanenden und abtragenden Werkzeugmaschinen. Springer, Berlin
2. <http://transregio96.de/>
3. Komanduri R, Hou ZB (2001) Thermal modeling of the metal cutting process, part III: temperature rise distribution due to the combined effects of shear plane heat source and the tool—chip interface. *Int J Mech Sci* 43:89–107
4. Davies MA, Ueda T, M'Saoubi R, Mullany B, Cooke AL (2007) On the measurement of temperature in material removal processes. *CIRP Ann Manuf Technol* 56(2):581–604
5. Tönshoff HK, Denkena B (2004) Spanen: Grundlagen. Springer, Berlin
6. König W (2008) Fertigungsverfahren 1: Drehen, Fräsen, Bohren. Springer, Berlin
7. Pabst R, Fleischer J, Michna J (2010) Modelling of the heat input for face-milling processes. *CIPR Ann* 59(1):121–124
8. Umbrello D, Filice L, Rizzuti S, Micari F, Settineri L (2007) On the effectiveness of finite element simulation of orthogonal cutting with particular reference to temperature prediction. *J Mater Process Technol* 189:284–291
9. Ustinov V, Kneer R, Al-Sibai F, Schulz SG, El-Magd E (2010) Influence of surface roughness on the contact heat transfer. 14th international heat transfer conference IHTC14, Washington, USA
10. Dix M (2013) Ressourceneffizientes Hochleistungsbohren mit Spiralbohrern—Analyse und Prozessgestaltung. Dissertation, TU Chemnitz
11. Klocke F, Bergs T, Busch M, Rohde L, Witty M, Cabral GF (2011) Integrated approach for a knowledge-based process layout for simultaneous 5-axis-milling of advanced materials. *Adv Tribol* 2:108–115
12. Drossel WG, Wittstock V, Bräunig M, Schmidt G (2013) Untersuchung der thermischen Werkzeugverformung. *wt-Werkstattstechnik online* 103(11/12)
13. <http://www.mscsoftware.com/product/marc>
14. Arrazola PJ, Özel T, Umbrello D, Davies M, Jawahir IS (2013) Recent advances in modelling of metal machining processes. *Ann CIRP Manuf Technol* 62(2):695–718
15. <http://www.deform.com/>
16. Jaspers SPFC, Dautzenberg JH (2002) Materials behaviour in conditions similar to metal cutting: flow stress in the primary shear zone. *J Mater Process Technol* 122:322–330